Enhanced vibrational resonance in a single neuron with chemical autapse for signal detection

Zhiwei He(何志威), Chenggui Yao(姚成贵), Jianwei Shuai(帅建伟), and Tadashi Nakano
Citation: Chin. Phys. B, 2020, 29 (**12**): 128702. DOI: 10.1088/1674-1056/abb7
Journal homepage: http://cpb.iphy.ac.cn; http://iopscience.iop.org/cpb

What follows is a list of articles you may be interested in

Cross-frequency network analysis of functional brain connectivity in temporal lobe epilepsy

Hai-Tao Yu(于海涛), Li-Hui Cai(蔡立辉), Xin-Yu Wu(武欣昱), Jiang Wang(王江), Jing Liu(刘静), Hong Zhang(张宏)
Chin. Phys. B, 2019, 28 (**4**): 048702. DOI: 10.1088/1674-1056/28/4/048702

Effect of stochastic electromagnetic disturbances on autapse neuronal systems

Liang-Hui Qu(曲良辉), Lin Du(都琳), Zi-Chen Deng(邓子辰), Zi-Lu Cao(曹子露), Hai-Wei Hu(胡海威)
Chin. Phys. B, 2018, 27 (**11**): 118707. DOI: 10.1088/1674-1056/27/11/118707

Firing dynamics of an autaptic neuron

Wang Heng-Tong, Chen Yong
Chin. Phys. B, 2015, 24 (**12**): 128709. DOI: 10.1088/1674-1056/24/12/128709

Effects of channel noise on synchronization transitions in delayed scale-free network of stochastic Hodgkin-Huxley neurons

Wang Bao-Ying, Gong Yu-Bing
Chin. Phys. B, 2015, 24 (**11**): 118702. DOI: 10.1088/1674-1056/24/11/118702

Adaptive synchronization control of coupled chaotic neurons in the external electrical stimulation

Yu Hai-Tao, Wang Jiang, Deng Bin, Wei Xi-Le, Chen Ying-Yuan
Chin. Phys. B, 2013, 22 (**5**): 058701. DOI: 10.1088/1674-1056/22/5/058701

Enhanced vibrational resonance in a single neuron with chemical autapse for signal detection*

Zhiwei He(何志威)[1], Chenggui Yao(姚成贵)[2,†], Jianwei Shuai(帅建伟)[3,‡], and Tadashi Nakano[4]

[1]*Department of Mathematics, Shaoxing University, Shaoxing* 312000, *China*
[2]*College of Mathematics, Physics and Information Engineering, Jiaxing University, Jiaxing* 314000, *China*
[3]*Department of Physics, State Key Laboratory of Cellular Stress Biology, Innovation Center for Cell Signaling Network, Xiamen University, Xiamen* 361102, *China*
[4]*Graduate School of Frontier Biosciences, Osaka University,* 5408570, *Japan*

(Received 16 July 2020; revised manuscript received 9 August 2020; accepted manuscript online 14 September 2020)

Many animals can detect the multi-frequency signals from their external surroundings. The understanding for underlying mechanism of signal detection can apply the theory of vibrational resonance, in which the moderate high frequency driving can maximize the nonlinear system's response to the low frequency subthreshold signal. In this work, we study the roles of chemical autapse on the vibrational resonance in a single neuron for signal detection. We reveal that the vibrational resonance is strengthened significantly by the inhibitory autapse in the neuron, while it is weakened typically by the excitatory autapse. It is generally believed that the inhibitory synapse has a suppressive effect in neuronal dynamics. However, we find that the detection of the neuron to the low frequency subthreshold signal can be improved greatly by the inhibitory autapse. Our finding indicates that the inhibitory synapse may act constructively on the detection of weak signal in the brain and neuronal system.

Keywords: neuronal dynamics, autapse, vibrational resonance, synchronization, time delay

PACS: 87.19.lj, 05.45.Xt, 87.19.lm **DOI:** 10.1088/1674-1056/abb7f9

1. Introduction

The multi-frequency signals are prevalent and act an important role in biology.[1–3] For hunting and communication, many animals can receive and send out signals with different amplitudes and frequencies. For instance, the high frequency signal with a low frequency envelope is more common in the weakly electric fish who communicates with electric signal with a high frequency about 500–1000 Hz, while the low frequency signals (< 20 Hz) are resulted from external environment and small prey items. These signals can be sensed by the electroreceptors located on the skin surface, which is importance for the fish's electro-communication, navigation, and electrolocation.[4] Middleton reported a high frequency signal compounded by a low frequency envelope transmission in a electrosensory system,[5] and the response of the pyramidal cell to a high-frequency signal with the social envelope has also been investigated in weakly electric fishes.[6] To understand how animals succeed in getting the useful information from the hybrid signals, the neuronal system responding to the high frequency signal with a low frequency envelope has been widely investigated.

Indeed, the detection of weak signal is a challenging task,[7,8] because weak signal may be concealed easily by noise. However, the finding of stochastic resonance shows that noise can improve greatly the detection of subthreshold signal in many nonlinear systems.[9,10] Similar to the role of noise in stochastic resonance, the high-frequency signal has a similar effect.[11–13] The response of a system to the subthreshold signal with a low frequency can be amplified by the optimal amplitude of the high-frequency signal. This phenomenon was first observed in 2000, and is called a vibrational resonance.[11] Since multi-frequency signals are ubiquitous in many fields, vibrational resonance has been intensively investigated also.[14–18] The vibrational resonance has been discussed in the CA1 neuron model[19] and the relationship between vibrational resonance and phase locking in Hodgkin–Huxley model was investigated.[20] It is of great significance to understand the detection of a weak signal in a nonlinear system, and so the effects of stochastic resonance and vibrational resonance have been widely investigated and analyzed in the single neuron[21–23] and the neuronal networks.[24–29]

As a major structural connection in neuronal systems, synapses also play an extraordinary effect in information propagation, which are classified into electrical synapse and chemical synapse. Autapse, as a special synapse, has been found originally in neocortex by Van der Loos and Glaser in 1972.[30] The autapse, which connects a neuron to itself by a branch of its own axon, has been evidenced in the cerebellum, striatum, hippocampus, and neocortex.[31,32] Since then, many studies

*Project supported partially by the National Natural Science Foundation of China (Grant Nos. 11675112, 11705116, 11675134, and 11874310) and the National Natural Science Foundation of China for the 111 Project (Grant No. B16029).

†Corresponding author. E-mail: yaochenggui2006@126.com
‡Corresponding author. E-mail: jianweishuai@xmu.edu.cn

have revealed that the autapses have a significant impact on brain functions. For example, Bekkers found that the excitatory autapses can maintain persistent electrical activity in the cerebral cortex.[33] The artificial GABAergic autaptic conductances can enhance the precision of firing time in pyramidal neurons,[34] and elevate the threshold of evoking action potentials to inhibit the repetitive firing.[35] As a fact, a plethora of interesting phenomena have been found with the effect of autapse in the neuronal networks.[36–48]

In this work, motivated by the biological function of autapse mentioned above, we study the effects of autapse on the response of a single neuron to external multi-frequency signals. Similar work about the effect of autapse on signal transmission in the neuronal network was discussed in our paper.[49] We here are interested in the problem how the inhibitory autapse enhances signal detection and information processing in a signal neuron? Thus, we will investigate the effect of chemical autapse on vibrational resonance in a signal neuron level. We show that the vibrational resonance can be enhanced greatly by an inhibitory autapse for signal detection, while weakened vibrational resonance is observed in the neuron with an excitatory autapse. Such an observation contradicts a popular view that the inhibitory synapse plays typically a suppressive role in neuronal dynamics.[50,51]

The structure of the paper is as follows. In Section 2, a mathematical model for a neuron with an autapse is introduced, and a quantitative measurement for vibrational resonance is also included. Section 3 presents the main numerical results. Finally, Section 4 give our conclusions and discussion.

2. Model

To reveal the effect of autapse on the neuronal dynamics, we will investigate vibrational resonance in the Hodgkin–Huxley neuron model, the equations are written as[52]

$$\begin{aligned} C_{\rm m}\frac{{\rm d}V}{{\rm d}t} &= -(g_{\rm K}n^4(V-V_{\rm K})+g_{\rm Na}m^3h(V-V_{\rm Na}) \\ &\quad +g_{\rm l}(V-V_{\rm l}))+I_{\rm aut}+I_0+I_{\rm stimu}, \qquad (1a)\\ \frac{{\rm d}m}{{\rm d}t} &= \alpha_m(1.0-m)-\beta_m m, \qquad (1b)\\ \frac{{\rm d}n}{{\rm d}t} &= \alpha_n(1.0-n)-\beta_n n, \qquad (1c)\\ \frac{{\rm d}h}{{\rm d}t} &= \alpha_h(1.0-h)-\beta_h h, \qquad (1d) \end{aligned}$$

where C_m is the cell capacitance, V represents the membrane potential of neuron, $g_{\rm Na}$, $g_{\rm K}$, and g_l correspond to the maximum conductances of the sodium, potassium, and leak currents, respectively. $V_{\rm K}$, $V_{\rm Na}$, and $V_{\rm l}$ stand for the potassium, sodium, and leakage reversal potentials, respectively. I_0 is a stimulus current. $I_{\rm stimu}=A\cos(\omega t)+B\cos(\Omega t)$ is the multi-frequency periodic signal, the frequency ratio $N=\Omega/\omega$. The m and h are gating variables which control the activation and inactivation of the sodium current, the gating variable n regulates the activation of the potassium current. These dynamics of the gating variables are controlled by the voltage-dependent rates $\alpha_x(V)$ and $\beta_x(V)$ $(x=m,n,h)$, which read

$$\begin{aligned} \alpha_m &= \frac{0.1(V+40)}{1-{\rm e}^{-(V+40)/10}}, \qquad (2a)\\ \beta_m &= 4{\rm e}^{(-V-65)/18}, \qquad (2b)\\ \alpha_n &= \frac{0.01(V+55)}{1-{\rm e}^{-(V+55)/10)}}, \qquad (2c)\\ \beta_n &= 0.125{\rm e}^{-(V+65)/80}, \qquad (2d)\\ \alpha_h &= 0.07{\rm e}^{-(V+65)/20}, \qquad (2e)\\ \beta_h &= \frac{1.0}{1+{\rm e}^{-(V+35)/10}}. \qquad (2f) \end{aligned}$$

The $I_{\rm aut}$ is an additional delayed stimulus which stands for the self-feedback current. We only study the effect of the excitatory chemical and inhibitory chemical autapse since it was found in experiment. The electrical autapse is not considered in our work. Different models have been proposed to simulate the chemical synapse, such as the fast threshold modulation (FTM) scheme,[53] the sigmoidal function model,[54] and the exponential function model.[55,56] In the paper, we use the chemical autaptic current with monoexponential functions which is fitted by experimental data,[57] it is written as

$$I_{\rm aut}=-G(t-\tau)(V-V_{\rm syn}). \qquad (3)$$

Here $G(t-\tau)$ is the autaptic conductance function, τ represents the time delay, and $V_{\rm syn}$ is the autaptic reversal potential. For excitatory synapse, $V_{\rm syn}$ is larger than the resting potential for generating an inward current. For inhibitory synapse, $V_{\rm syn}$ is close to potassium's reversal potential.[55] As a result, the values of $V_{\rm syn}=0.0$ mV and $V_{\rm syn}=-80.0$ mV for excitatory and inhibitory synapses are typically used in research, respectively.[56,58] The equation of autaptic conductance is modeled as

$$G(t)=g_{\rm syn}\alpha(t-t_{\rm fire}), \qquad (4)$$

with

$$\alpha(t)=\frac{t}{t_{\rm d}}{\rm e}^{-\frac{t}{t_{\rm d}}}, \qquad (5)$$

where $t_{\rm fire}$ ($\sim$ ms) is the spiking time of the neuron, $g_{\rm syn}$ is the maximum conductance of the autaptic channel, and the parameter $t_{\rm d}=2.0$ ms represents the decay time of the function. Table 1 presents the values of the parameters in our model.

To determine the response of the neuron to a low frequency signal, we calculate Q defined by

$$\begin{aligned} Q &= \sqrt{Q_{\rm s}^2+Q_{\rm c}^2},\\ Q_{\rm s} &= \frac{2}{nT}\int_{T_0}^{T_0+nT}V(t)\sin(\omega t)\,{\rm d}t,\\ Q_{\rm c} &= \frac{2}{nT}\int_{T_0}^{T_0+nT}V(t)\cos(\omega t)\,{\rm d}t, \qquad (6) \end{aligned}$$

where $T=2\pi/\omega$. We have chosen large values for the tran-

sient evolution T_0 and the average time T with $n = 500$. Clearly, the signal transfer is optimized when the output firing is synchronized by the low frequency signal. Thus, there is a very large value of Q when such a synchronization occurs.[19,20] It is noteworthy that the value of Q is a proportional function of the Fourier transform coefficient $F(\omega')$ at $\omega' = \omega$ ($F(\omega') = \int_0^{+\infty} e^{-i\omega' t} V(t)\,dt$). The advantage of calculation of Q is that it is convenient and fast. As a fact, we have also calculated the Fourier transform spectrum at ω, and it does not change the results.

Table 1. Parameter values.

Parameter	Description	Value
C_m	cell membrane capacitance	1.0 mF/cm^2
g_{Na}	the maximum conductance for sodium	120.0 mS/cm^2
g_K	the maximum conductance for potassium	36.0 mS/cm^2
g_l	the maximum leakage conductance	0.3 mS/cm^2
V_K	the reversal potential for potassium	−77.0 mV
V_{Na}	the reversal potential for sodium	50.0 mV
V_l	leakage reversal potential	−54.0 mV
I_0	the constant stimulus current	1.0 μA/cm^2
V_{syn}	the autaptic reversal potential	0.0 or −80.0 mV
τ	time delay	0–10 ms
g_{syn}	the maximum conductance of autaptic channel	0–6 mS/cm^2
A	the amplitude of weak signal	1.0 μA/cm^2
B	the amplitude of high-frequency force	0–600 μA/cm^2
ω	the frequency of weak signal	0.5 ms^{-1}
Ω	the frequency of high-frequency force	0.6–10 ms^{-1}

3. Results

First, we investigate the effect of chemical autapse on the response of a single neuron to the low frequency signal. Figures 1(a) and 1(b) illustrate the value of Q versus B with excitatory and inhibitory autapse and without autapse. For the rows from top, middle to bottom, $\Omega = 1.5, 3\sqrt{3}$, and 10.0, respectively. For the columns from left to right, $\tau = 2.0$ and 5.0, respectively. In the paper, $g_{syn} = 0.0$ indicates non-autapse. One can see that Q increases with increasing amplitude B and then decreases after reaching to a maximum, indicating clearly the phenomenon of vibrational resonance. Interestingly, we find that the values of Q for the neuron with inhibitory autapse become larger than those without autapse, and the resonance windows for the optimal value of B with $Q > 25$ get wider, and the optimal response window for vibrational resonance is shifted to the higher values of B. The inhibitory autapse can enhance the response of the neuron to the low-frequency subthreshold signal [Fig. 1(a)]. Whereas the value of Q is very small for the excitatory autapse (solid green circles). From these figures, one can also find that the strengthening effect of inhibitory autapse on vibrational resonance is general, no matter what value of the frequency ratio $N = \Omega/\omega$ is.

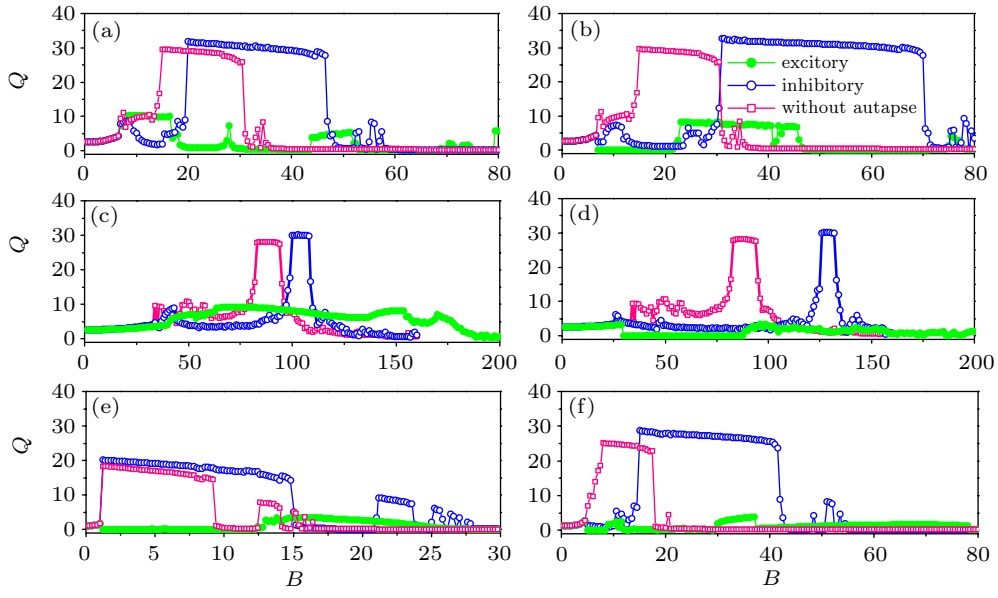

Fig. 1. (a)–(f) The response Q of neuron against B without autapse ($g_{syn} = 0.0$) and with excitatory and inhibitory autapses for different parameter settings of τ and Ω. $\Omega = 1.5, 3\sqrt{3}$, and 10.0 corresponds to the top, middle, and bottom rows, respectively, For the left and right columns, $\tau = 2.0$ and 5.0, respectively. Here, $g_{syn} = 5.0$.

To compare globally the deferent effects of excitatory autapse and inhibitory autapse on vibrational resonance, the dependency of Q on amplitude B and time delay τ is shown for excitatory and inhibitory autapses in Fig. 3, where the color wine represents the occurrence of vibrational resonance with large value of Q (i.e., $Q > 25$). From the series of $V(t)$ of neuron without autpase in Fig. 2, we find $Q > 25$ ($Q = 16.76$ when $B = 14.5$, $Q = 29.49$ when $B = 16$.) stands for the situation that the spiking of the neuron is synchronous with the low-frequency signal. In the paper we suggest that $Q > 25$ stands for the situation that the information of the low-frequency signal can be detected. From Fig. 3, the multiple vibrational resonance which depends sensitively on τ and B is observed clearly for neurons with excitatory or inhibitory autapse. Comparing any three subfigures in each row, however, we find that the size of resonance region which is marked by wine is much bigger for the neuron with the inhibitory autapse than that with the excitatory autapses, showing a stronger response of the neuron with inhibitory autapse to the low frequency signal. Furthermore, we find that the size of the wine region decreases with increasing $g_{\rm syn}$ for the excitatory autapses, indicating that vibrational resonance is not favored with excitatory autapses.

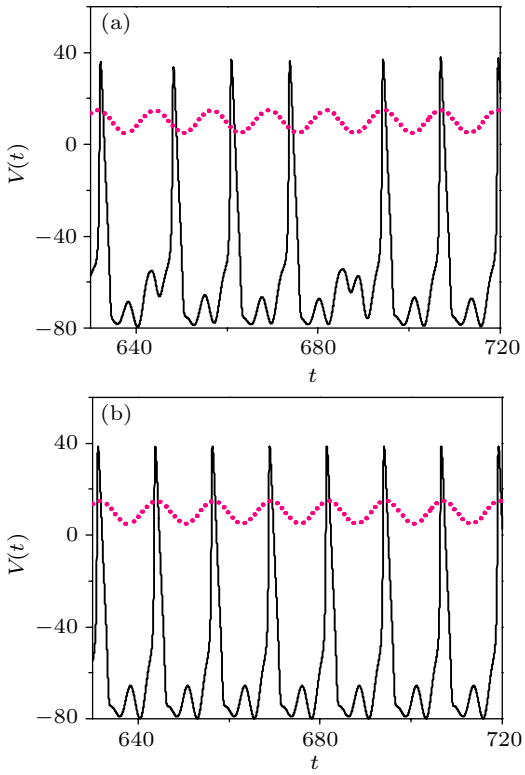

Fig. 2. (a)–(b) Time series of $V(t)$ of neuron without autapse ($g_{\rm syn} = 0.0$) for $B = 14.5$ and 16, respectively. $\omega = 0.5$ and $\Omega = 1.5$.

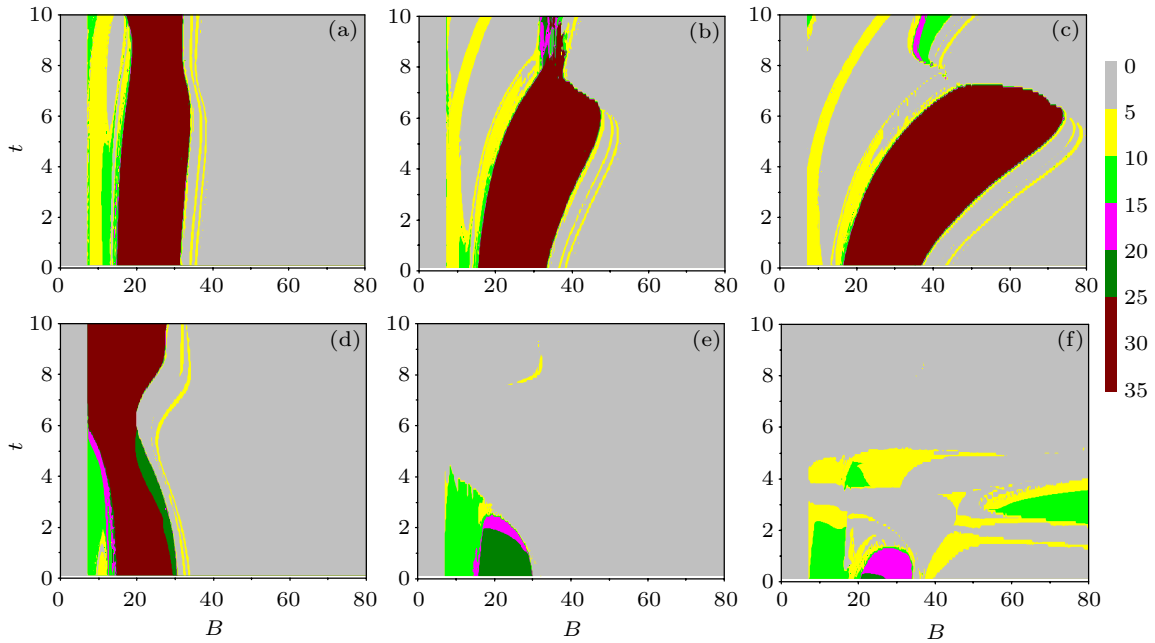

Fig. 3. Contour plots of Q as a function of B and τ in a neuron with (a)–(c) inhibitory autapse and (d)–(f) excitatory autapse, respectively. From left column to the right column, $g_{\rm syn} = 0.4$, 2.0, and 5.0, respectively. Here, $\omega = 0.5$ and $\Omega = 1.5$.

To gain a deeper understanding of the inhibitory-autapse-enhanced vibrational resonance, figure 4 presents the dependence of $T_{\rm i}$, which is defined as the inter-spike interval as a function of B, for inhibitory (Figs. 4(a)–4(c)) and excitatory autapses (Figs. 4(d)–4(f)). For the columns from left, middle, to right in Fig. 4, $g_{\rm syn} = 0.4$, 2.0, and 5.0, respectively. From these figures, one can find that $T_{\rm i}$ is multi-valued, indicating aperiodic spiking activities. We have checked carefully the data of $T_{\rm i}$, but could not find period doubling or expansion with parameter changes. We can observe clearly that some periodical synchronization states occur for excitatory and inhibitory autapses with $\omega/\omega' = 1:1$ or $3:2$, where ω' is defined as the frequency of spiking. Interestingly, comparing the three subfigures in each row with increasing $g_{\rm syn}$, the periodic synchronization window for $\omega/\omega' = 1:1$ (i.e., frequency synchronization) gets longer for the neuron with the inhibitory autapse,

while such frequency synchronization is destroyed for the neuron with excitatory autapse. The figures in the middle column show that $T_{\rm i}$ decreases tardily to T ($T = 2\pi/\omega = 12.56$) with increasing B, which results in the synchronization of the neuron with low-frequency subthreshold signal in the resonance interval.

Further, we show the dynamical phase diagrams on the (B, τ) space for excitatory (Figs. 5(a)–5(c)) and inhibitory (Figs. 5(d)–5(f)) autapses with $g_{\rm syn} = 0.4, 2.0$, and 5.0 respectively. Based on the observation of spiking, the neuron exhibits three primary features: non-exciting state (NE), aperiodic state (AS), and phase locking state (PL). In Fig. 5, the green region corresponds to AS state, the gray region stands for NE state in which the potential $V(t)$ fluctuates around a steady state, and the PL states for $\omega/\omega' = 3:2, 3:4, 1:2$, and $1:1$ (frequency synchronization) are marked by dark cyan, pink, yellow, and wine, respectively. The other ratios are marked by orange. Comparing Fig. 5 with Fig. 3, one can find that the regions

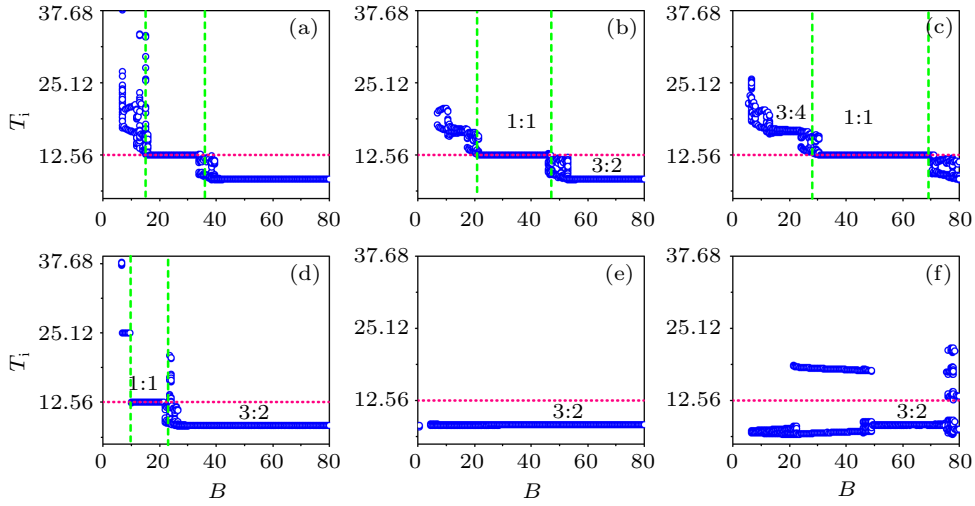

Fig. 4. (a)–(f) The bifurcation diagrams of $T_{\rm i}$ which is the interval time of serial spiking. The upper and lower rows correspond to the inhibitory and excitatory autapses, respectively. From the left column to the right column, $g_{\rm syn} = 0.4$, 2.0, and 5.0, respectively. Here $\tau = 5.0, \omega = 0.5$, and $\Omega = 1.5$.

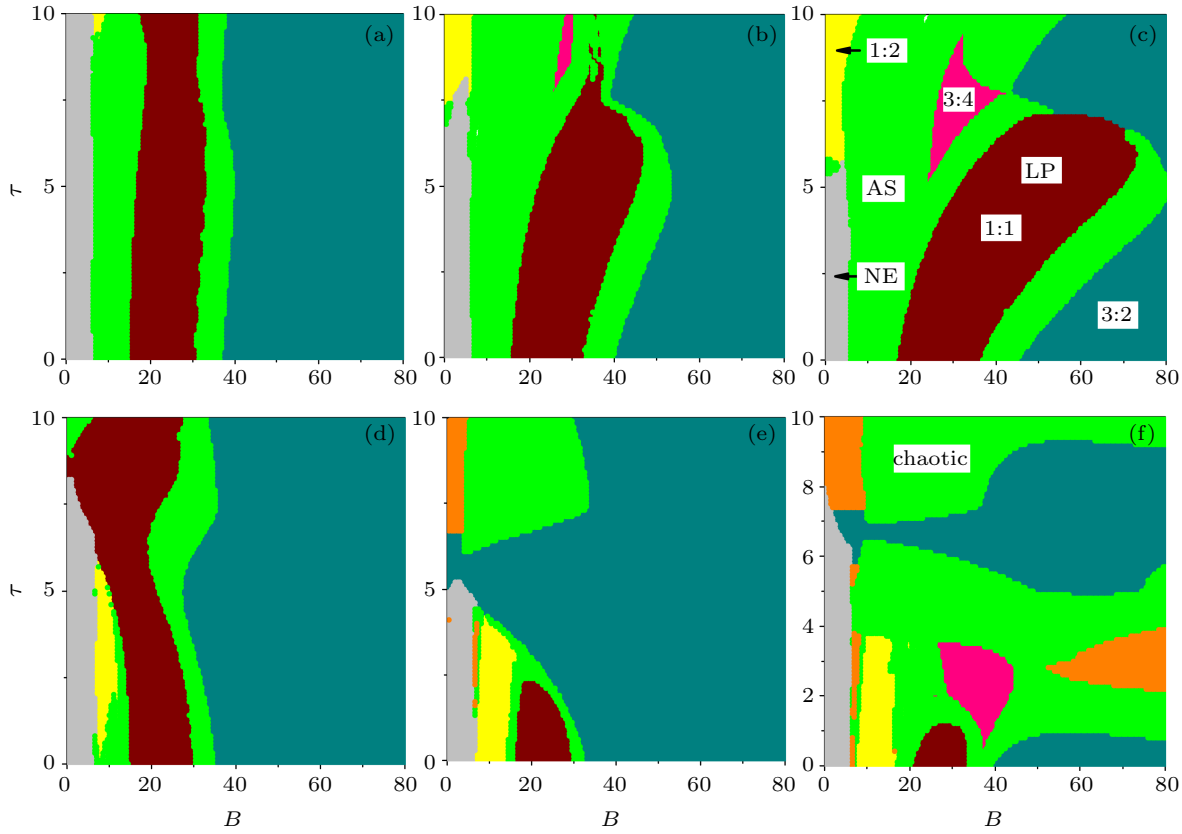

Fig. 5. The dynamical phase diagram on the (B, τ) space with (a)–(c) inhibitory and (d)–(f) excitatory autapses for $g_{\rm syn} = 0.4, 2.0$, and 5.0 (for left, middle, and right columns), respectively. The letters AS stand for aperiodic state. The letters NE represent non-exciting state where the potential $V(t)$ fluctuates around the steady state. The 1 : 1, 1 : 2, and 3 : 2 are locking ratios. Here, $\omega = 0.5$ and $\Omega = 1.5$.

with high value of Q (wine region) are almost the same as those of frequency synchronization, which can be enhanced by the inhibitory autapse, and depend on τ and B. This result suggests that the strengthening effect of inhibitory autapse on vibrational resonance results from the frequency synchronization.

Then, we explore the effect of the maximum conductance of autapse $g_{\rm syn}$ on the size of the synchronization region in (B,τ) space with the rational or irrational ratio of Ω/ω. To quantify the synchronization region, we introduce a normalized scaling factor $R = S_{\rm FS}/S$, where $S_{\rm FS}$ stands for the area of the synchronization region, and S represents the total area of (B,τ) space with $[0,80]\times[0,10]$ (a), $[0,200]\times[0,10]$ (b), and $[0,600]\times[0,10]$ (c), respectively. The results are shown in Fig. 6 for $\Omega = 1.5$, $3\sqrt{3}$, and 10.0. For excitatory autapse, R decreases to a small value with the increase of $g_{\rm syn}$. Thus, the strong excitatory autapse does not favor the frequency synchronization. Differently, R holds on a large value for the arbitrary autaptic weight $g_{\rm syn}$. The strengthen effect of inhibitory autapse on frequency synchronization is verified again.

Finally, we focus on the regions with a large Ω, and discuss the effects of frequency Ω on vibrational resonance and frequency synchronization for the neuron. Figures 7(a) and 7(b) give the normalized scaling factor R as a function of ratio $N = \Omega/\omega$ for $g_{\rm syn} = 2.0$ and 5.0, respectively. As shown in Fig. 7, multiple peaks of factor R are located at integer numbers for excitatory and inhibitory autapses, suggesting that there exists a resonance to the high-frequency force at the driving frequency. One can also find in Fig. 7 that the values of

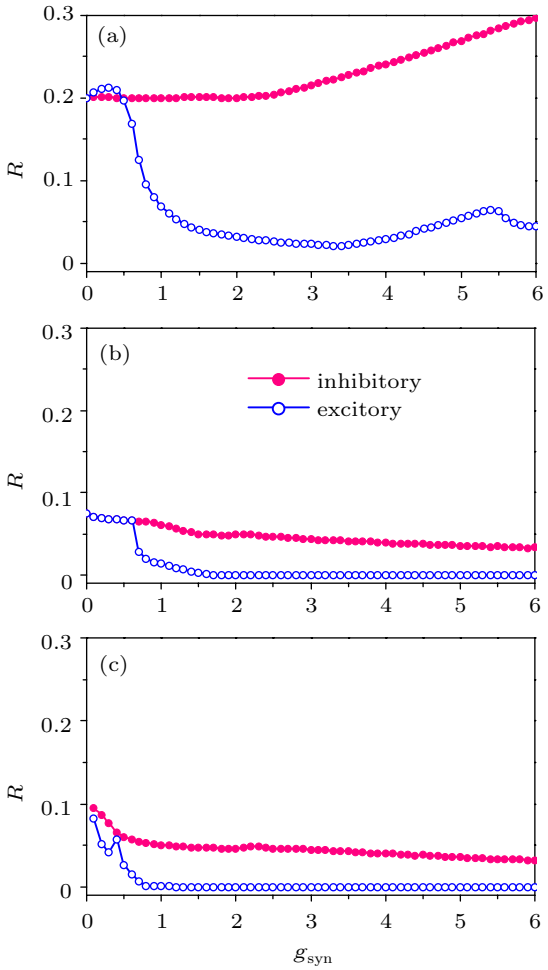

Fig. 6. The normalized scaling factor R against $g_{\rm syn}$ for $\Omega = 1.5$ (a), $3\sqrt{3}$ (b), and 10.0 (c) with excitatory and inhibitory autapses, respectively. Here, $\omega = 0.5$.

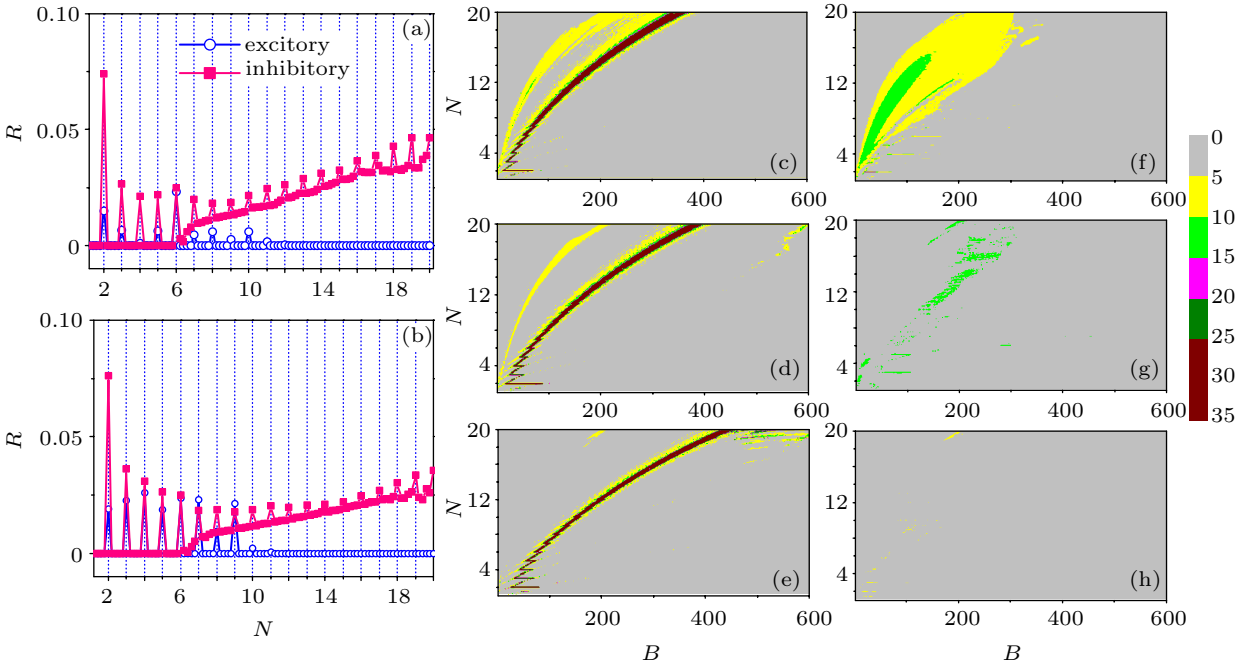

Fig. 7. The normalized factor $R = S_{\rm FS}/S$ in (τ,B) space as a function of Ω for $g_{\rm syn} = 2.0$ (a) and 5.0 (b), respectively, where $S_{\rm FS}$ is the area of region of 1 : 1 phase locking mode, and S is the area of (B,τ) space with $[0,600]\times[0,10]$. The circles and squares stand for excitatory and inhibitory autapses, respectively. (c)–(h) Contour plots of Q against B and N ($N = \Omega/\omega$) for (c)–(e) inhibitory autapse and (f)–(h) excitatory autapse with different N, respectively. From top column to bottom column, $\tau = 1.0$, 3.0, and 5.0, respectively. Here, $g_{\rm syn} = 5.0$ and $\omega = 0.5$.

peaks for the inhibitory autapse are larger than those for the excitatory autapses at the special frequencies with integer number. Besides these peaks, with the increase of N, the envelope of R for the inhibitory autapse increases when N is over a critical value, while R for the excitatory autapse vanishes. One also finds inhibitory autapse enhanced vibrational resonance for the large ratio N. Figures 7(c)–7(h) show the two-dimensional contour plots of Q as a function of B and N with inhibitory autapse (Figs. 7(c)–7(e)) and excitatory autapse (Figs. 7(f)–7(h)), respectively. From these figures, the strengthened vibrational resonance can also be observed for the arbitrary Ω with inhibitory autapses, while the weakened effect of excitatory autapse on the vibrational resonance can be verified for the general and incommensurable frequency Ω, and the VR with sensitive frequency dependence is justified.

4. Conclusions

We studied in detail the effects of excitatory and inhibitory autapses of a single neuron on the response to the multi-frequency signal. The vibrational resonance can be observed in such a neuron with different autapses, and sensitively depends on system's parameters. Surprisingly, the resonance response of the neuron with an inhibitory autapse becomes stronger than that without autapse. The resonance window gets wider with the inhibitory autapse, while the resonance region is reduced with the excitatory autapse. Thus the vibrational resonance is enhanced by the inhibitory autapse, indicating a strengthened detection of the neuron to the low-frequency signal.

The phase-locking is one of the best known phenomena in the nonlinear system with periodic stimulus. It has been shown that the vibrational resonance can be induced by phase-locking modes in the excitable system.[20] The vibrational resonance closely relates with the frequency matching relationship between the neuron with low frequency signal, which is called phase-locking induced vibrational resonance. We find that the inhibitory autapse can achieve 1 : 1 phase-locking mode, which leads to the enhanced vibrational resonance. However, the strong excitatory autapse exterminates the 1 : 1 phase-locking mode. The enhancement of vibrational resonance by the inhibitory autapse is of great interest and may be helpful for us to understand the dynamics of biological systems. Our results present a method to effectively detect the low-frequency signal for neurons with autapse.

The autapse has been found in 80% of cortical pyramidal neurons.[59] The biological function of autapse has attracted many researchers' interest and has been extensively investigated. For example, the self-adaption to stimulus can be strengthened by the autapse which is formed due to the contribution of the injury of the neuron.[60] The bursting oscillation can be inhibited by the autapse, indicating the improvement of the adaptive ability of neurons.[61] However, what is the role of the autapse in the brain and neural systems is still not completely comprehended. Although the finding of inhibitory-autapse-enhanced vibrational resonance is based on a purely numerical study in the paper, the constructive role of inhibitory autapse on neuronal dynamics, including the vibrational resonances, may be expected to be observed in experiment.

Data availability statements

The data used to support the findings of this study are available from the corresponding author on reasonable request.

References

[1] Maksimov A 1997 *Ultrasonics* **35** 79
[2] Victor J D and Conte M M 2000 *Vis. Neurosci.* **17** 959
[3] Gherm V, Zernov N, Lundborg B and Vastberg A 1997 *J. Atmos. Sol. Terr. Phys.* **59** 1831
[4] Heiligenberg W 1991 *Neural Nets in Electric Fish* (Cambridge: MIT Press)
[5] Middleton J, Longtin A J B and Maler L 2006 *Proc. Natl. Acad. Sci. USA* **103** 14596
[6] Stamper S A, Fortune E S and Chacron M J 2013 *J. Exp. Biol.* **216** 2393
[7] Wang G Y and Chen D J 1999 *IEEE Trans. Ind. Electron.* **46** 440
[8] Modestino J W and Ningo A Y 1979 *Trans. Inform. Theory.* **25** 592
[9] Wiesenfeld K and Moss F 1995 *Nature* **373** 33
[10] Gammaitoni L, Hanggi P, Jung P and Marchesoni F 1998 *Rev. Mod. Phys.* **70** 223
[11] Landa P S and McClintock P V E 2000 *J. Phys. A: Math. Gen.* **33** L433
[12] Baltanás J P, López L, Blechman I I, Landa P S, Zaikin A, Kurths J and Sanjuán M A F 2003 *Phys. Rev. E* **67** 066119
[13] Blekhman I I and Landa P S 2004 *Int. J. Non-Linear Mech.* **39** 421
[14] Ullner E, Zaikin A, Garcíía-Ojalvo J, Bascones R and Kurths J 2003 *Phys. Lett. A* **312** 348
[15] Casado-Pascual J and Baltanás J P 2004 *Phys. Rev. E* **69** 046108
[16] Yao C G Liu Y and Zhan M 2011 *Phys. Rev. E* **83** 061122
[17] Yao C G and Zhan M 2010 *Phys. Rev. E* **81** 061129
[18] Chizhevsky V N, Smeu E and Giacomelli G 2003 *Phys. Rev. Lett.* **91** 220602
[19] Wu X X, Yao C G and Shuai J W 2015 *Sci. Rep.* **5** 7684
[20] Yang L J, Liu W H, Yi M, Wang C J, Zhu Q M, Zhan X and Jia Y 2012 *Phys. Rev. E* **86** 016209
[21] Kaplan D T, Clay J R, Manning T, Glass L, Guevara M R and Shrier A 1996 *Phys. Rev. Lett.* **76** 4074
[22] He Z W and Yao C G 2020 *Sci. China Tech. Sc.* **63** 2339
[23] Yao C G, He Z W, Luo J M and Shuai J W 2015 *Phys. Rev. E* **91** 052901
[24] Wang L, Zhang P M, Liang P J, Pei J and Qiu Y H 2014 *Chin. Phys. Lett.* **31** 070501
[25] Ozer M, Uzuntarla M, Kayikcioglu T and Graham L 2008 *J. Phys. Lett. A* **373** 964
[26] Liang L S, Zhang J Q and Liu L Z 2014 *Chin. Phys. Lett.* **31** 050502
[27] Yu Y G, Wang W, Wang J F and Liu F 2001 *Phys. Rev. E* **63** 021907
[28] Zhang X, Huang H B, Li P J, Wu F P, Wu W J and Jiang M 2012 *Chin. Phys. Lett.* **29** 120501
[29] Cao B, Guan L N and Gu H G 2018 *Acta Phys. Sin.* **67** 240502 (in Chinese)
[30] Van Der Loos H and Glaser E M 1972 *Brain Res.* **48** 355
[31] Bekkers J M 1998 *Curr. Biol.* **8** R52
[32] Flight M H 2009 *Nat. Rev. Neurosci.* **10** 316
[33] Bekkers J M 2003 *Curr. Biol.* **13** R433
[34] Bacci A and Huguenard J R 2006 *Neuron* **49** 119
[35] Bacci A, Huguenard J R and Prince D A 2003 *J. Neurosci.* **23** 859
[36] Yi M and Yao C G 2020 *Complexity* **2020** 1292417
[37] Qin H X, Ma J, Wang C N and Wu Y 2014 *PLoS One* **9** e100849
[38] Wei C L and Zhao X 2019 *Chin. Phys. B* **28** 013201
[39] Usha K and Subha P A 2019 *Chin. Phys. B* **28** 020502
[40] Li D X, Bing J and Ye L Y 2019 *Acta Phys. Sin.* **68** 180502 (in Chinese)
[41] Li Y, Schmid G and Haggi P 2010 *Phys. Rev. E* **82** 061907

[42] Chen J X, Zhang H, Qiao Li Y, Liang H and Sun W G 2018 *Commun. Nonlinear Sci. Numer. Simulat.* **54** 202
[43] Yu H T, Cai L H, Wu X Y, Wang J, Liu J and Zhang H 2019 *Chin. Phys. B* **28** 048702
[44] Yao C G, He Z W, Nakano T and Shuai J W 2018 *Chaos* **28** 083112
[45] Song X L, Wang H T and Chen Y 2019 *Nonlinear Dyn.* **96** 2341
[46] Chen J X, Xiao J, Qian L Y and Xu J R 2018 *Nonlinear Sci. Numer. Simul.* **59** 331
[47] Ma J and Tang J 2019 *Sci. China Tech. Sc.* **62** 2038
[48] Lv M, Ma J, Yao Y G and Alzahrani F 2015 *Sci. China Tech. Sc.* **58** 448
[49] Yao C G He Z W and Nakano T 2019 *Nonlinear Dyn.* **97** 1425
[50] Qian N 1990 *Proc. Natl. Acad. Sci. USA* **87** 8145
[51] Eccles J C 1982 *Annu. Rev. Neurosci.* **5** 325
[52] Hodgkin A L and Huxley A F 1952 *J. Physiol.* **117** 500
[53] Burić N, Todorović K and Vasović N 2008 *Phy. Rev. E* **78** 036211
[54] Belykh I, Lange E and Hasler M 2005 *Phy. Rev. Lett.* **94** 188101
[55] Schutter E D 1988 *Computational Modeling Methods for Neuroscientists* (Cambridge: MIT Press)
[56] Wang S T, Wang W and Liu F 2006 *Phys. Rev. Lett.* **96** 018103
[57] Connelly W M and Lees G 2010 *J. Physiol.* **588** 2047
[58] Ozera M, Perc M, Uzuntarla M and Koklukayab E 2010 *NeuroReport* **21** 338
[59] Lübke J, Markram H, Frotscher M and Sakmann B 1996 *J. Neurosci.* **16** 3209
[60] Wang C N, Guo S L, Xu Y, Ma J, Tang J Alzahrani F and Aatef H 2017 *Complexity* **2017** 5436737
[61] Xu Y, Ying H P, Jia Y, Ma J and Hayat T 2017 *Sci. Rep.* **7** 43452